Title Page

A laboratory specific scaling factor to predict the in vivo human clearance of aldehyde oxidase substrates

Authors:

Mailys De Sousa Mendes[1#], Alexandra Orton[2], Helen E. Humphries[1], Barry Jones[2], Iain Gardner[1], Sibylle Neuhoff[1], and Venkatesh Pilla Reddy[3*#]

Address:

[1]Certara UK Limited, Simcyp Division, Sheffield, UK (MDSM, HEH, IG, SN)

[2]Research & Early Development, Oncology R&D, AstraZeneca, Cambridge, UK (AO, BJ)

[3]Modelling and Simulation, Research & Early Development, Oncology R&D, AstraZeneca, Cambridge, UK (VPR)

 # V.P.R and M.D.S.M are joint first authors

*Corresponding author: Dr. Venkatesh Pilla Reddy Ph.D

Address: Modelling and Simulation, Research & Early Development, AstraZeneca, Hodgkin Building c/o B310, Cambridge Science Park, Milton Road, Cambridge, Cambridgeshire, CB4 0WG, UK

Tel: +44 (0)7742645481

Email: venkatesh.reddy@astrazeneca.com

DMD-AR-2020-000082R1

Running Title Page

Running title: Scaling factors for aldehyde oxidase substrates

No. of text pages: 33

No. of tables: 3

No. of figures: 6

No. of references: 38

Abstract word count: 248

Introduction word count: 414

Discussion word count: 993

Abbreviations: ADME, absorption, distribution, metabolism, and excretion; ASA, automated sensitivity analysis; AUC, are under curve; C_{max}, maximum concentration; CYP, Cytochrome P450; CL, clearance; CL_{int}, intrinsic clearance; AO, Aldehyde oxidase; fu, unbound fraction in plasma; fu_{inc}, unbound fraction in the incubation; fm, fraction metabolized; HLM, human liver microsomes; IVIVE, *in vitro-to-in vivo* extrapolation; LC-MS/MS, liquid chromatography-tandem mass spectrometry; B/P: blood/plasma ratio; NCE, New Chemical Entity; PBPK, Physiologically based pharmacokinetic; PK Pharmacokinetics; V_{ss}, volume of distribution at steady state.

2

Abstract:

Aldehyde oxidase (AO) efficiently metabolizes a range of compounds with N-containing heterocyclic aromatic rings and/or aldehydes. The limited knowledge of AO activity and abundance (*in vitro* and *in vivo*) has led to poor prediction of *in vivo* systemic clearance (CL) using *in vitro*-to-*in vivo* extrapolation (IVIVE) approaches, which for drugs in development can lead to their discontinuation. We aimed to identify appropriate scaling factors (SF) to predict AO CL of future New Chemical Entities (NCE). The metabolism of six AO substrates was measured in human liver cytosol (HLC) and S9 fractions. Measured blood-to-plasma ratios and free fractions (in the *in vitro* system and in plasma) were used to develop physiologically-based pharmacokinetic (PBPK) models for each compound. The impact of extrahepatic metabolism was explored, and the intrinsic clearance required to recover *in vivo* profiles was estimated and compared to *in vitro* measurements. Using HLC data and assuming only hepatic metabolism, a systematic underprediction of clearance was observed (average fold under-prediction was 3.8). Adding extrahepatic metabolism improved the accuracy of the results (average fold error of 1.9). A workflow for predicting metabolism of an NCE by AO is proposed, an empirical (lab-specific) SF of 3 on the predicted CL_{IV} allows a reasonable prediction of the available clinical data. Alternatively, considering also extrahepatic metabolism, a SF of 6.5 applied on the intrinsic clearance ($CL_{int,AO}$) could be used. Future research should focus on the impact of the *in vitro* study designs and the contribution of extrahepatic metabolism to AO-mediated clearance to understand the mechanisms behind the systematic under-prediction.

Significance Statement

This works describes the development of scaling factors to allow *in vitro-in vivo* extrapolation of the clearance of compounds by aldehyde oxidase metabolism in humans. In addition, PBPK models were developed for each of the AO substrate compounds investigated.

DMD-AR-2020-000082R1

Introduction

Aldehyde oxidase (AO) is a cytosolic molybdenum-containing enzyme that very efficiently oxidizes a range of N-containing heterocyclic aromatic rings and aldehydes (Montefiori et al., 2017). The limited knowledge about AO activity, abundance, and translation from *in vitro* to *in vivo* has led to poor prediction of *in vivo* clearance (CL) and consequently to clinical failure of some AO substrates (Fan et al., 2016; Jensen et al., 2017). The reasons for the poor prediction of CL of aldehyde oxidase substrates (CL_{AO}) are multiple: Firstly, AO is only expressed in the cytosol, and therefore standard metabolism studies using human liver microsomes (HLM) will overlook AO metabolism (Obach, 2011; Zientek and Youdim, 2015; Dalvie and Di, 2019). Secondly, scaling from animal data can be challenging as dogs have low AO expression and the AO expression in different rat strains is very variable (Dalvie et al., 2013; Tanoue et al., 2013). Additionally although monkey, rat, and rabbit AO have been investigated, the metabolism of compounds by AO in these species only moderately overlaps with human clearance by AO (Al salhen, 2014; Dick, 2018) Finally, the inter-individual variability in AO expression in humans is high and consequently the risk of having data for a non-representative individual is considerable (Hutzler et al., 2014). In 2010, Zientek *et al*. have predicted the *in vivo* $CL_{int,AO}$ from *in vitro* data and compared it to the $CL_{int,AO}$ estimated after IV administration for 5 compounds (Zientek et al., 2010). The $CL_{int,AO}$ was underestimated by 13-fold (range: 5-32) when using human liver cytosol (HLC) data, and by 15-fold (range: 3-52) when using Human Liver S9 (HLS9) data. Strategies have been formulated to handle AO mediated clearance in drug discovery and development. However, understanding why human *in vivo* clearance is under-predicted using *in vitro* $CL_{int,AO}$ from HLC and HLS9 is necessary to understand the role of AO in the metabolism of new chemical entities in a wider chemical space.

In this work, we aimed (1) to assess the prediction of intravenous (IV) clearance of six AO substrates from *in vitro* data, then (2) to derive an empirical scaling factor (SF) that (3) could be used to predict the CL of future NCE using Physiologically-Based Pharmacokinetic (PBPK) modelling. Initially the metabolism by AO was assumed to occur only in the liver and results from HLC and HLS9 were

4

DMD-AR-2020-000082R1

compared. However, there is compelling evidence of extrahepatic metabolism (CL_{IV} greater than the hepatic blood flow, and AO expression data in extrahepatic tissues); hence, also the impact of extrahepatic metabolism was explored. Finally scaling factors were estimated to optimally recover *in vivo* concentration-time profiles.

DMD-AR-2020-000082R1

Materials and Methods

Pooled (150 donors; lot No.38289) human liver cytosol, pooled (150 donors: lot No. 3829) human liver S9, and pooled (150 donors; equal gender mix) human liver microsomes were obtained from Corning Life Sciences (Woburn, MA). It is possible that the human donor liver tissues might have been perfused or preserved with University of **Wisconsin** solution or another allopurinol-containing buffer, which may exhibit aldehyde oxidase inhibition potential at high concentrations.

Frozen human plasma (pooled from 78 individuals, mixed gender) generated using K2-EDTA as an anticoagulant was purchased from BioreclamationIVT (Baltimore, MD). AO substrates O^6-benzylguanine, zaleplon, zoniporide, and carbazeran were sourced from Sigma-Aldrich (Poole, UK). BIBX1382 was sourced from Santa Cruz Biotechnology (Dallas, TX). Ziprasidone was synthesized at AstraZeneca (Cambridge, UK). Formic acid (FA), ammonium formate and dimethylsulfoxide (DMSO) were purchased from Sigma-Aldrich (Poole, UK). HPLC grade methanol, water and acetonitrile (ACN) were obtained from Thermo Fisher Scientific (Waltham, MA). All other solvents were HPLC grade and, unless otherwise specified, all other reagents were purchased from Sigma-Aldrich (Poole, UK).

Compound selection

The aim of this work was to assess the robustness of the prediction of CL_{AO}. To remove the additional uncertainty associated with predicting processes influencing oral bioavailability, only drugs with reported IV clearance and a fraction metabolized by AO (fm_{AO}) of greater than 5% were selected for inclusion in this exercise. Using these criteria, the involvement of AO in the metabolism of O6-benzylguanine, BIBX1382, carbazeran, zaleplon, ziprasidone, and zoniporide was investigated in this study. Physicochemical data including molecular weight, logP and pKa, acid/base nature as well as blood binding properties and information about the compound elimination were compiled for all drugs (Table 1). When data from several reliable sources were available a weighted mean value was used.

Determination of aldehyde oxidase metabolic CL_{int}:

6

The AO-mediated metabolism was measured in incubations containing either a HLC suspension at 1 mg protein/mL or Human Liver S9 (HLS9) suspension at 2.5 mg protein/ml, both in Phosphate buffer (100 mM), pH7.4. The reactions were initiated by addition of pre-diluted compounds (2.5 µl from 100 µM in 100 mM Phosphate buffer /ACN/DMSO 90/9/1) to give a final nominal concentration of 1 µM. The solvent concentration did not exceed a total of 0.1%. The samples were then incubated at 37°C for either 120 minutes in HLC or 60 minutes in HLS9 with time points taken at 10, 30, 60, 90, 120 and 5, 10, 20, 40, 60 minutes, respectively. The aliquots (25 µl) were precipitated with ACN (1 in 5 v/v) containing internal standard (historic AstraZeneca compound; AZ10024306), centrifuged at 3500 rpm for 10 minutes and the supernatant diluted 1 in 7 (v/v) with ultra-pure HPLC water before analysis by LC-MS/MS. All incubations were carried out in duplicate. The *in vitro* elimination rate constant corresponding to parent compound depletion was determined for each reaction using the 1st order decay calculation in Microsoft Excel Sheet.

Determination of unbound fraction in human plasma (fu):

The extent of binding of compounds to plasma proteins was determined by equilibrium dialysis at a compound concentration of 5 µM using the Rapid Equilibrium Device (RED; Thermoscientific Pierce). Phosphate buffer (100 mM, pH 7.4) was added to the buffer chamber, and 300 µl of plasma spiked with compound to the sample chamber. The unit was covered with a gas permeable lid and incubated for 18 hours at 37°C at 300 rpm with 5% CO_2. At the end of incubation, samples (50 µl) from both buffer and plasma chambers were removed for analysis. Samples and standards were matrix matched and analyzed using LC-MS/MS. The unbound fraction in plasma (fu) was calculated as follows:

$$fu = \frac{\text{Concentration in buffer chamber}}{\text{Concentration in plasma chamber}} \quad Eq\ (1)$$

DMD-AR-2020-000082R1

Determination of blood-to-plasma ratio (B/P):

A volume of plasma sufficient for the assay was obtained from whole human blood by centrifugation (3,220 g for 10 minutes at 4°C). The test compound (10 µM) was added to 398 µl of the pre-warmed human plasma and blood separately and incubated for 30 minutes. After incubation, the blood samples were centrifuged for 10 minutes at 3,220 g (37°C) and the plasma samples stored at 37°C. Aliquots (400 µl) of ice-cold acetonitrile containing internal standard were added to 100 µl samples of plasma separated from centrifuged whole blood and to reference plasma samples. These samples were then centrifuged, diluted with distilled water, and analyzed by LC-MS/MS to determine the compound concentration. B/P was calculated as follows:

$$B/P \ = \ \frac{\text{Concentration in reference plasma}}{\text{Concentration in plasma from blood}} \quad Eq\ (2)$$

Determination of unbound fraction in HLM (fu$_{mic}$):

The extent of binding of compounds to HLM was determined by equilibrium dialysis using the HT Dialysis LLC device (Gales Ferry, CT) with HLM at a concentration of 1 mg protein/ml and a final compound concentration of 1 µM. PBS (150 µl) was added to the buffer well and 150 µl HLM containing the compound to the sample well and incubated at 37°C for 4 hours. After the incubation, 50-µl aliquots from both donor and receiver wells were removed for analysis. Samples and standards were matrix matched and analyzed by LC-MS/MS. The unbound fraction in the incubation (fu$_{mic}$) was calculated as follows:

$$Fu_{mic} = \frac{\text{Conc. in buffer well}}{\text{Conc. in microsmal suspension well}} \quad Eq\ (3)$$

LC-MS/MS analysis:

The concentration of all compounds in the incubations was determined by LC-MS/MS. An Acquity ultra performance liquid chromatography (UPLC) system, (Waters, UK) coupled to a triple-

DMD-AR-2020-000082R1

quadrupole mass spectrometer (Xevo TQ-S; Waters, Milford, MA) was used to carry out the sample analysis. The details of quantification of analytes is described in **Supplementary Text.** Detection of the ions was performed in the MRM mode. Peak integration and calibrations were performed using TargetLynx software (Version 4.1, Waters, Milford, MA).

Prediction of IV clearance using PBPK models:

The clinical trials providing the reference CL_{IV} have been conducted in subjects with variable demographic characteristics (i.e. age range, proportion of females, healthy/cancer patients). The specific demographics will influence some of the physiological parameters (i.e. liver weight, plasma protein concentration) that in turn can impact the PK parameters observed. Therefore, PBPK models were developed for each drug using the Simcyp Simulator V18R2 and the simulated trial designs and virtual population were selected accordingly to match the observed clinical trial (Table 1) (Kaye et al., 1984; Dolan et al., 1998; Rosen et al., 1999; Tserng et al., 2003; Miceli et al., 2005; Hutzler et al., 2012; Dalvie et al., 2013)

The Intrinsic clearance (CL_{int}) obtained *in vitro* from HLC and HLS9 fractions were corrected by the free fraction in the *in vitro* assay. The free fraction in HLM have been measured using 1 mg/ml of microsomal protein. No clear trend concerning the difference in binding between HLC and HLM was observed, therefore the binding was assumed to stay the same in HLC and HLS9 fraction (Cubitt, 2009). When the protein concentrations used were different from the 1 mg/mL assessed in the binding experiments, the free fraction was extrapolated using the equation from Austin *et al*. (Austin et al., 2002).

The B/P, fu and fu_{mic}, and *in vitro* metabolism data were used to develop PBPK models for each compound (Table 1). The main plasma binding protein was assumed to be albumin for the acid, neutral, and ampholyte compounds and alpha-1 acid glycoprotein for the basic compounds. Physicochemical properties were gathered from literature sources and whole body PBPK models with predicted volumes of distribution calculated using the Rodgers and Rowlands method were

9

DMD-AR-2020-000082R1

developed [3]. The contribution of microsomal metabolism, renal and biliary excretion to the clearance was added to the PBPK models when applicable (Table 1).

Aldehyde oxidase is present in organs other than the liver (Moriwaki et al., 2001; Nishimura and Naito, 2006). To study the potential impact of extra-hepatic metabolism, the activity per mg of cytosolic protein in the kidney was assumed to be the same as that of the liver and the free intrinsic activity was scaled based on the human cytosolic protein per gram of kidney (CPPGK), kidney weight, and blood flow. A CPPGK value of 40.6 mg/g was used (Scotcher). Similarly, lung metabolism was also explored and the activity per mg of cytosolic protein was assumed to be the same as that of the liver. The IVIVE scaling approach (Figure 2) using the well-stirred lung model is integrated within the Simcyp Simulator and was simply entered as additional lung clearance, it was calculated with the following scaling parameters: cytosolic protein per gram of lung (CPPGLu) yield of 20 mg/g, a lung tissue weight (excluding blood) of 550 g and a cardiac output of 386 L/h. CPPGLu was obtained using the S9 fraction in the lung of 28 mg/g tissue (Kozminski et al., 2018) and assuming that the fraction of cytosolic protein to S9 protein is constant between the lung, liver, and kidney. Due to the limited expression of AO in the intestine (Moriwaki et al., 2001; Nishimura and Naito, 2006; Hutzler et al., 2012), intestinal metabolism was not considered in the current analysis.

A linear regression between the predicted CL_{IV} (Dose/$AUC_{0-infinity}$ after a simulated single IV dose) and the observed CL_{IV} was calculated using R (version 3.5.1, www.r-project.org), with a weighting option of 1/Y_pred to avoid bias toward the highest clearance value.

A sensitivity analysis was done on the AO intrinsic clearance of the 6 drugs to explore the impact of increasing the intrinsic clearance in the liver and in extrahepatic organs on the predicted CL_{IV}. In the sensitivity analyses described here, the kidney was used as a surrogate organ to account for all the extrahepatic metabolism in the body. The kidney was chosen as the site of extrahepatic metabolism for practical reasons rather than splitting the clearance over several different organs. The ratio between the observed and predicted CL_{IV} was calculated.

The intrinsic clearance of each compound was then optimized using available PK profiles, except for

BIBX1382 where no concentration-time profile was available and only the clearance is reported in

the literature. The following dosing regimens were used to simulate the PK profiles: O6-

benzylguanine – bolus administration of 20 mg/m^2 to 7 cancer patients aged 45-74 years (prop. of

female = 0.42) ((Tserng et al., 2003); carbazeran – 10 min infusion of 1.28 mg/kg of carbazeran to 7

healthy male volunteers aged 20-50 years (Kaye et al., 1984); zaleplon – 30 min infusion of 5 mg to

10 healthy subjects aged 30-32 years (prop. of female = 0.5) (Rosen et al., 1999); ziprasidone – 1 h

infusion of 5 mg to 13 male subjects aged 19-37 years (Miceli et al., 2005); zoniporide - 1 h infusion

of 80 mg to 4 male healthy subjects aged 18-55 years (Dalvie et al., 2010). Additionally, the Kp scalar

were optimized for carbazeran (=0.13) and zoniporide (=0.45) to better fit the observed V$_{ss}$. The

required (in silico) intrinsic clearance from the PBPK model was then compared to the measured (in

vitro) intrinsic clearance to calculate a scaling factor for each compound.

Additionally, to verify the usefulness of this approach in predicting clearance of a new compound an

average scaling factor was applied to the *in vitro* intrinsic clearance of the studied drugs. The

average scaling factor was calculated based on all the drugs except the one that was being

predicted.

Results

The investigated compounds covered a wide range of fm_{AO}, ranging from 0.064 (ziprasidone) to 0.98 (carbazeran). The log P values ranged from 1.04 (O^6-Benzylguanine) to 3.97 (BIBX1382) and there was one neutral, 4 basic compounds, and an ampholyte. Table 1 summarizes the physicochemical data and the measured $CL_{int,u}$ values obtained in HLC, HLS9, and HLM. The results were overall in good agreement with literature data, except for ziprasidone where the HLC $CL_{int,u}$ was more than 10-fold lower than previously reported values (33.4 vs 410.3 µL/min/mg (Obach et al., 2012)) (Table 2).

Prediction of IV clearance using PBPK models.

Figure 3 compare the observed CL_{IV} to the CL_{IV} predicted from the PBPK model (Table 1).

HLC Liver only

Using HLC data the average extent of underprediction of CL_{IV} was 3.8 and ranged from 1.9 to 5.2 (Figure 3). The best prediction was obtained for BIBX1382 (1.9 fold) and the biggest difference was for ziprasidone (5.2 fold). A coefficient of 2.77 was obtained using a weighted linear regression between the observed clearance and predicted clearance. For all the compounds the average coefficient of variation (CV%) for CL predicted by the PBPK models was 26% (range: 15.9-37.5%). The predicted variability was in accordance with the mean observed CV of 21% (range: 5.7 to 35.9%). The Figure 4 shows that no trend between the extend of underestimation and the predicted fraction metabolized (fm) by AO could be observed.

HLS9 Liver only

Using HLS9 experiment the CL_{IV} was predicted to be lower than CL_{IV} obtained from HLC with an average extent of underprediction of 5.8 and it ranged from 2.9 (BIBX1382) to 10.6 (Zaleplon) (Figure 3). A coefficient of 4.02 was obtained using a weighted linear regression between the observed clearance and predicted clearance. Simcyp workspaces for these 6 compounds using HLS9 data are provided as supplementary datasets 1 to 6.

12

HLC Liver and Kidney

When the metabolism in the liver and the kidney were included (assuming the same intrinsic clearance per mg of cytosolic protein) a small improvement of the prediction of the CL_{IV} was observed. The extent of underprediction of CL_{IV} was 3.5 and ranged from 1.4 (BIBX1382) to 5.2 (ziprasidone) (Figure 3). A coefficient of 2.26 was obtained using a weighted linear regression between the observed clearance and predicted clearance.

HLC Liver, Kidney, and Lung

When the metabolism in the liver, the kidney and the lung were included (assuming the same activity per mg of cytosolic protein) a more pronounced increase in the accuracy of prediction of the CL_{IV} was observed. The average extent of underprediction of CL_{IV} was 3.2 and ranged from 0.9 (BIBX1382) to 5.2 (ziprasidone) (Figure 3). A coefficient of 1.74 was obtained using a weighted linear regression between the observed clearance and predicted clearance.

Sensitivity analyses

Figure 5 shows the sensitivity analyses made on a scaling factor applied to the intrinsic clearance and considering the metabolism in liver and kidney. O^6-benzylguanine and zaleplon have similar profile and reach the observed CL_{IV} with a scaling factor of around 15, BIXB1382 quickly reaches a clearance close to the observed clearance but also become quickly non sensitive to any changes in $CL_{int,u}$. Carbazeran reaches a plateau around 75% of the observed CL_{IV}, the blood flow is the limiting factor in this case. Ziprasidone $CL_{int,u}$ was significantly lower value than reported in the literature (Table 2) and even with a 20-fold increase in the intrinsic clearance the observed CL_{IV} is not attained. Zoniporide CL_{IV} reaches the observed CL_{IV} with a scaling factor of 3.5.

PK profiles

13

Figure 6 shows the simulated profiles with and without optimization compared to the observed CL_{IV}. The intrinsic clearance ($CL_{int, AO}$) and scaling factor obtained are reported in Table 2. In this study an average $CL_{int, AO}$ scaling factor of 6.5 was necessary to recover the PK profiles. Ziprasidone has a low fm_{AO} and the metabolic activity was lower in this study than previously reported and for this reason ziprasidone was excluded from the calculation of the average scalar analysis.

Table 3 shows that using the average scalar factor from the other drugs significantly improves the prediction of CL_{IV}, with an average underprediction of 1.5 (range 0.98-1.96). All drugs were predicted within a 2-fold error which is considered adequate for predictions early in drug discovery. Applying the scaling factor of 6.5 to ziprasidone the CL_{IV} was underpredicted by 3.9-fold increasing the average fold underprediction to 1.9 for the six compounds.

DMD-AR-2020-000082R1

Discussion

Using IVIVE approaches to predict aldehyde oxidase mediated clearance has typically resulted in a significant underprediction of the observed clearance resulting in the clinical failure of multiple drugs that are metabolized by AO (Fan et al., 2016; Jensen et al., 2017). This study explored IVIVE of CL_{AO} and aimed to develop a methodology to aid informed decision making on newly developed drug candidates that showed potential to be metabolized by AO and a workflow for AO-mediated clearance prediction is proposed. Overall, using HLC, the intravenous CL continued to be under estimated but HLC performed better than HLS9 in this study. Ideally the *in vitro* system of each laboratory should be characterized by measuring the $CL_{int,u}$ of the selected probe substrates present in this study, then a scaling factor should be calculated using the information in Table 2 and applied on the intrinsic clearance assuming metabolism in the liver and the kidney as explained in the method section. The coefficient obtained with the linear regression could also be applied as an empirical scalar directly on the CL_{IV}. If in-house probe substrate CL_{int} data are not available, a scalar of 4.6 could be applied on the $CL_{int,u}$ based on the literature published values of AO mediated metabolism.

Measured B/P and fu were like values reported in the literature (Alousi et al., 2007; Zientek et al., 2010; Akabane et al., 2012). The average *in vitro* intrinsic clearances obtained from the literature were overall higher especially for ziprasidone. One reason for this discrepancy in *in vitro* intrinsic clearances could be explained by the variability of activity in AO across human liver cytosolic fractions (Hutzler et al., 2014), or alternatively due to the nature of the experimental protocol (i.e. incubation and sampling time, buffer). It is possible that human donor liver tissues were preserved in allopurinol containing University of Wisconsin solution, may exhibit weak AO inhibitory effect at higher concentrations and could affect the scaling factors calculated in thus study. Nevertheless, Barr et al., have showed that small residual amounts of allopurinol or oxypurinol did not appear to impact AO activity (Barr et al., 2014). By analyzing the different protocols used in the literature no

15

clear association between experimental condition and measured CL_{int} was observed, a larger dataset or new specific *in vitro* assays looking at the impact of the protocol would be required (Dick, 2018).

In this data set the fraction metabolized by AO was estimated by including all known pathways; however, even if some inhibitors of aldehyde oxidase have been identified in vitro (Johns, 1967; Johnson et al., 1985; Obach, 2004), limited clinical drug interactions via inhibition of aldehyde oxidase have been recorded restricting the additional validation of *in -vivo* probe substrates or inhibitors for the verification of the fm_{AO} of given substrate.

Some compounds have an IV clearance higher than the hepatic blood flow suggesting extrahepatic elimination. Aldehyde oxidase is expressed in multiple tissues included the kidney (Moriwaki et al., 2001; Nishimura and Naito, 2006). A scenario assuming an AO activity/expression per mg of cytosolic protein in the kidney is identical to that in the liver was simulated in the PBPK models and even though an improved prediction was observed, the underprediction of CL was still significant. Expression of AO in the intestine is limited and incubations of AO substrate with human intestinal cytosol resulted in no measurable metabolism (Moriwaki et al., 2001; Nishimura and Naito, 2006; Hutzler et al., 2012) therefore, intestinal metabolism was not considered in the current analysis. The lung is a highly perfused organ with a significant tissue volume and an AO absolute abundance within 6-fold of that in the liver (Ezkurdia et al., 2015). Previous studies have attempted to incorporate lung metabolism into IVIVE approaches for AO mediated clearance (Kozminski et al., 2018) however, in this study the reported intrinsic activity in the lung was almost 1000-fold lower than in the liver explaining the absence of significant impact of lung metabolism on the overall predicted clearance (Kozminski et al., 2018). In this study even assuming a tissue activity per mg of lung cytosol identical to that in the liver did not explain the underestimation of clearance observed for all compounds (Figure 3).

Aldehyde oxidase has been shown to have a limited stability and freeze-thaw cycles might result in higher variability and therefore the metabolic activity might be underestimated in *in vitro* assays

(Sherratt and Damani, 1989; Hutzler et al., 2012). The underestimation of AO clearance is likely to be due to an underestimation of the intrinsic clearance as well as extrahepatic metabolism.

An additional way to scale from *in vitro* to *in vivo* would be to use the absolute abundance rather than activity per mg of protein. This approach would allow the use of recombinant AO and therefore to have an extremely specific system with less risk of contamination from other enzymes (i.e. Xanthine oxidase). In addition, the absolute abundance in all of the different tissues in the body could be accounted for with a single *in vitro* metabolism measurement. So far the absolute abundance in the liver has been measured (Barr et al., 2013; Fu et al., 2013; Ezkurdia et al., 2015; Wiśniewski et al., 2016) and recombinant AO are available. Unfortunately, there is a lot of variability between the different laboratories (mean: 34.5 pmol/mg of cytosolic protein; range: 1.41- 60.2 pmol/mg of cytosolic protein, 4 studies, a total of 30 livers) and the absolute abundance has not been measured in the recombinant systems.

An additional aim of this work was to gather the input information for PBPK models for the different AO substrate compounds so that the models could be available for use in future research efforts. The PBPK models could be used to investigate different aspects such as interindividual differences in AO expression, to study the interaction between AO substrates and inhibitors (e.g., between zaleplon and cimetidine (Dalvie and Di, 2019)) or to investigate the PK of these compounds in different populations of individuals.

Conclusion

A workflow for NCE metabolized by AO was suggested, an empirical scaling factor of 3 on the predicted CL_{IV} based on HLC data could be applied for NCEs that are significantly metabolized by AO when using PBPK models for predicting the exposure of NCE in the human. Alternatively, a scaling factor of 6.5 could be apply to the AO intrinsic clearance in the liver and kidney. Ideally each

laboratory should develop a correlation using a set of probe substrates under their own assay conditions; however, if the *in vitro* $CL_{int,u}$ for probe substrates are not available in a given laboratory an empirical scaling factor of 4.6 based on this work could be applied for $CL_{int,u}$ in HLC. Additional research on the impact of the *in vitro* study designs and extrahepatic metabolism is suggested to understand the mechanism behind the systematic underprediction observed for AO.

DMD-AR-2020-000082R1

Authorship Contributions

Participated in research design: De Sousa Mendes, Gardner, Neuhoff, and Pilla Reddy

Conducted experiments Orton, and Jones

Performed data analysis: Pilla Reddy and De Sousa Mendes

Wrote or contributed to the writing of the manuscript: De Sousa Mendes, Orton, Humphries, Jones, Gardner, Neuhoff, and Pilla Reddy

Conflicts of interest

Venkatesh Pilla Reddy, Alexandra Orton, and Barry Jones are full-time employees of AstraZeneca when this study was conducted and hold shares of AstraZeneca. Mailys De Sousa Mendes, Helen E. Humphries, Iain Gardner, and Sibylle Neuhoff employees of Certara UK Limited when this study was conducted.

References

Akabane T, Gerst N, Masters JN, and Tamura K (2012) A quantitative approach to hepatic clearance prediction of metabolism by aldehyde oxidase using custom pooled hepatocytes. *Xenobiotica; the Fate of Foreign Compounds in Biological Systems* **42:**863-871.

Al salhen KS (2014) In vitro oxidation of aldehyde oxidase from rabbit liver: Specificity toward endogenous substrates. *Journal of King Saud University - Science* **26:**67-74.

Alousi AM, Boinpally R, Wiegand R, Parchment R, Gadgeel S, Heilbrun LK, Wozniak AJ, DeLuca P, and LoRusso PM (2007) A phase 1 trial of XK469: toxicity profile of a selective topoisomerase IIbeta inhibitor. *Investigational New Drugs* **25:**147-154.

Austin RP, Barton P, Cockroft SL, Wenlock MC, and Riley RJ (2002) The Influence of Nonspecific Microsomal Binding on Apparent Intrinsic Clearance, and Its Prediction from Physicochemical Properties. *Drug Metabolism and Disposition* **30:**1497-1503.

Barr JT, Jones JP, Joswig-Jones CA, and Rock DA (2013) Absolute quantification of aldehyde oxidase protein in human liver using liquid chromatography-tandem mass spectrometry. *Molecular Pharmaceutics* **10:**3842-3849.

Cubitt HE (2009) In Vitro Assessment of Hepatic and Intestinal Conjugation Reactions

and Impact on Drug Clearance Prediction, in: *School of Pharmacy and Pharmaceutical Sciences*, University of Manchester.

Dalvie D and Di L (2019) Aldehyde oxidase and its role as a drug metabolizing enzyme. *Pharmacol Ther* **201:**137-180.

Dalvie D, Xiang C, Kang P, and Zhou S (2013) Interspecies variation in the metabolism of zoniporide by aldehyde oxidase. *Xenobiotica; the Fate of Foreign Compounds in Biological Systems* **43:**399-408.

Dalvie D, Zhang C, Chen W, Smolarek T, Obach RS, and Loi C-M (2010) Cross-Species Comparison of the Metabolism and Excretion of Zoniporide: Contribution of Aldehyde Oxidase to Interspecies Differences. *Drug Metabolism and Disposition* **38:**641-654.

Dick RA (2018) Refinement of In Vitro Methods for Identification of Aldehyde Oxidase Substrates Reveals Metabolites of Kinase Inhibitors. *Drug Metabolism and Disposition* **46:**846-859.

Dolan ME, Roy SK, Fasanmade AA, Paras PR, Schilsky RL, and Ratain MJ (1998) O6-benzylguanine in humans: metabolic, pharmacokinetic, and pharmacodynamic findings. *Journal of Clinical Oncology: Official Journal of the American Society of Clinical Oncology* **16:**1803-1810.

Ezkurdia I, Calvo E, Del Pozo A, Vázquez J, Valencia A, and Tress ML (2015) The potential clinical impact of the release of two drafts of the human proteome. *Expert Review of Proteomics* **12:**579-593.

Fan PW, Zhang D, Halladay JS, Driscoll JP, and Khojasteh SC (2016) Going Beyond Common Drug Metabolizing Enzymes: Case Studies of Biotransformation Involving Aldehyde Oxidase, γ-Glutamyl Transpeptidase, Cathepsin B, Flavin-Containing Monooxygenase, and ADP-Ribosyltransferase. *Drug Metabolism and Disposition: The Biological Fate of Chemicals* **44:**1253-1261.

Fu C, Di L, Han X, Soderstrom C, Snyder M, Troutman MD, Obach RS, and Zhang H (2013) Aldehyde oxidase 1 (AOX1) in human liver cytosols: quantitative characterization of AOX1 expression level and activity relationship. *Drug Metabolism and Disposition: The Biological Fate of Chemicals* **41:**1797-1804.

Hutzler JM, Yang Y-S, Albaugh D, Fullenwider CL, Schmenk J, and Fisher MB (2012) Characterization of aldehyde oxidase enzyme activity in cryopreserved human hepatocytes. *Drug Metabolism and Disposition: The Biological Fate of Chemicals* **40:**267-275.

Hutzler JM, Yang Y-S, Brown C, Heyward S, and Moeller T (2014) Aldehyde oxidase activity in donor-matched fresh and cryopreserved human hepatocytes and assessment of variability in 75 donors. *Drug Metabolism and Disposition: The Biological Fate of Chemicals* **42:**1090-1097.

20

Jensen KG, Jacobsen A-M, Bundgaard C, Nilausen DØ, Thale Z, Chandrasena G, and Jørgensen M (2017) Lack of Exposure in a First-in-Man Study Due to Aldehyde Oxidase Metabolism: Investigated by Use of 14C-microdose, Humanized Mice, Monkey Pharmacokinetics, and In Vitro Methods. *Drug Metabolism and Disposition: The Biological Fate of Chemicals* **45:**68-75.

Johns DG (1967) Human liver aldehyde oxidase: differential inhibition of oxidation of charged and uncharged substrates. *The Journal of Clinical Investigation* **46:**1492-1505.

Johnson C, Stubley-Beedham C, and Stell JG (1985) Hydralazine: a potent inhibitor of aldehyde oxidase activity in vitro and in vivo. *Biochemical Pharmacology* **34:**4251-4256.

Kaye B, Offerman JL, Reid JL, Elliott HL, and Hillis WS (1984) A species difference in the presystemic metabolism of carbazeran in dog and man. *Xenobiotica; the Fate of Foreign Compounds in Biological Systems* **14:**935-945.

Kozminski KD, Heyward S, and Zientek M (2018) Aldehyde Oxidase Activity in Human Vascular Tissue and its Potential Contribution to Extra-hepatic Metabolism, in: *ISSX*.

Lake BG, Ball SE, Kao J, Renwick AB, Price RJ, and Scatina JA (2002) Metabolism of zaleplon by human liver: evidence for involvement of aldehyde oxidase. *Xenobiotica; the Fate of Foreign Compounds in Biological Systems* **32:**835-847.

Liu X, Wang J-Q, and Zheng Q-H (2005) Lipophilicity coefficients of potential tumor imaging agents, positron-labeled O(6)-benzylguanine derivatives. *Biomedical chromatography: BMC* **19:**379-384.

Miceli JJ, Wilner KD, Swan SK, and Tensfeldt TG (2005) Pharmacokinetics, Safety, and Tolerability of Intramuscular Ziprasidone in Healthy Volunteers. *The Journal of Clinical Pharmacology* **45:**620-630.

Montefiori M, Jørgensen FS, and Olsen L (2017) Aldehyde Oxidase: Reaction Mechanism and Prediction of Site of Metabolism. *ACS omega* **2:**4237-4244.

Moriwaki Y, Yamamoto T, Takahashi S, Tsutsumi Z, and Hada T (2001) Widespread cellular distribution of aldehyde oxidase in human tissues found by immunohistochemistry staining. *Histology and Histopathology* **16:**745-753.

Nishimura M and Naito S (2006) Tissue-specific mRNA expression profiles of human phase I metabolizing enzymes except for cytochrome P450 and phase II metabolizing enzymes. *Drug Metabolism and Pharmacokinetics* **21:**357-374.

Obach RS (2004) Potent inhibition of human liver aldehyde oxidase by raloxifene. *Drug Metabolism and Disposition: The Biological Fate of Chemicals* **32:**89-97.

Obach RS (2011) Predicting clearance in humans from in vitro data. *Curr Top Med Chem* **11:**334-339.

Obach RS, Prakash C, and Kamel AM (2012) Reduction and methylation of ziprasidone by glutathione, aldehyde oxidase, and thiol s-methyltransferase in humans: an in vitro study. *Xenobiotica* **42:**1049-1057.

Renwick AB, Ball SE, Tredger JM, Price RJ, Walters DG, Kao J, Scatina JA, and Lake BG (2002) Inhibition of zaleplon metabolism by cimetidine in the human liver: in vitro studies with subcellular fractions and precision-cut liver slices. *Xenobiotica; the Fate of Foreign Compounds in Biological Systems* **32:**849-862.

Rosen AS, Fournié P, Darwish M, Danjou P, and Troy SM (1999) Zaleplon pharmacokinetics and absolute bioavailability. *Biopharmaceutics & Drug Disposition* **20:**171-175.

Roy SK, Korzekwa KR, Gonzalez FJ, Moschel RC, and Dolan ME (1995) Human liver oxidative metabolism of O6-benzylguanine. *Biochemical Pharmacology* **50:**1385-1389.

Scotcher D Physiological scaling factors and Mechanistic models for prediction of Renal clearance from in vitro data, Faculty of Medical and Human Sciences Manchester, University of Manchester.

Sherratt AJ and Damani LA (1989) Activities of cytosolic and microsomal drug oxidases of rat hepatocytes in primary culture. *Drug Metabolism and Disposition: The Biological Fate of Chemicals* **17:**20-25.

Tanoue C, Sugihara K, Uramaru N, Watanabe Y, Tayama Y, Ohta S, and Kitamura S (2013) Strain difference of oxidative metabolism of the sedative-hypnotic zaleplon by aldehyde oxidase and cytochrome P450 in vivo and in vitro in rats. *Drug Metabolism and Pharmacokinetics* **28:**269-273.

Tracey WR, Allen MC, Frazier DE, Fossa AA, Johnson CG, Marala RB, Knight DR, and Guzman-Perez A (2003) Zoniporide: A Potent and Selective Inhibitor of the Human Sodium-Hydrogen Exchanger Isoform 1 (NHE-1). *Cardiovascular Drug Reviews* **21:**17-32.

Tserng K-Y, Ingalls ST, Boczko EM, Spiro TP, Li X, Majka S, Gerson SL, Willson JK, and Hoppel CL (2003) Pharmacokinetics of O6-benzylguanine (NSC637037) and its metabolite, 8-oxo-O6-benzylguanine. *Journal of Clinical Pharmacology* **43:**881-893.

Wiśniewski JR, Wegler C, and Artursson P (2016) Subcellular fractionation of human liver reveals limits in global proteomic quantification from isolated fractions. *Analytical Biochemistry* **509:**82-88.

Zientek M, Jiang Y, Youdim K, and Obach RS (2010) In vitro-in vivo correlation for intrinsic clearance for drugs metabolized by human aldehyde oxidase. *Drug Metabolism and Disposition: The Biological Fate of Chemicals* **38:**1322-1327.

Zientek MA and Youdim K (2015) Reaction phenotyping: advances in the experimental strategies used to characterize the contribution of drug-metabolizing enzymes. *Drug Metab Dispos* **43:**163-181.

DMD-AR-2020-000082R1

Legend for Figures

Figure 1. Chemical structure of aldehyde oxidase substrate that have reported IV clearance.

Figure 2. In vitro-in vivo extrapolation for scaling AO metabolism in the lung

Figure 3. Predicted CL_{IV} (+/- standard deviation) compared to mean observed CL_{IV} (+/- standard deviation). Results are compared to the unity line and 2- and 5-fold bias lines. SF: Scaling factor.

Figure 4. Fold underprediction of Clearance when considering only hepatic metabolism compared to the predicted fm_{AO}.

Figure 5. Sensitivity analyses on the intrinsic activity of AO in HLC assuming metabolism in the liver and the kidney.

Figure 6. Simulated mean profile with the default input in black (5th-95th percentile in grey) and after optimization in blue (5th-95th percentile in dashed light blue) assuming metabolism in the liver and kidney, compared to observed concentrations (open circles). A: Administration of a single 20mg/m2 dose of O^6-Benzylguanine in IV bolus to 7 cancer patients aged 45-74 (prop. Female = 0.42) (15); B: Administration of a single 1.28 mg/kg IV infusion of carbazeran over 10 min to 7 healthy male volunteers aged 20-50 years (12); C: Administration of a single 5 mg IV infusion of zaleplon over 30 min to 10 healthy subjects aged 30-32 years (prop. Female= 0.5) (14); D: Administration of a single 5 mg IV infusion of ziprasidone over 1h to 13 male subjects aged 19-37 years (13); E: Administration of a single 80 mg IV infusion of zoniporide over 1h to 4 male healthy subjects aged 18-55 years (22).

DMD-AR-2020-000082R1

Table 1: PBPK model input parameters and Clinical data used for PBPK model verification

Compound	O[6]-Benzylguanine	BIBX1382	Carbazeran	Zaleplon	Ziprasidone	Zoniporide
Phys chem						
MW (g/mol)	241.25	387.84	360.41	305.33	412.94	320.35
logP	1.04 (Liu et al., 2005)	3.97 [a]	1.83 [a]	1.3 [a]	4.53 [a]	1.15 [a]
Compound type	ampholyte	diprotic base	base	neutral	diprotic base	diprotic base
pka	9.35;3.361 [a]	2.83;8.64 [a]	8.6 [a]	-	6.31; 8.24 [a]	3.4;7.2 (Tracey et al., 2003)
B/P	0.9 [a]	1.45 [a]	0.735 [a]	0.853	0.63 [a]	0.938 [a]
fu	0.14 [a]	0.12 [a]	0.09 [a]	0.576 [a]	0.001 [a]	0.421 [a]
Main binding protein	HSA[b]	AGP[b]	AGP[b]	HSA[b]	AGP [b]	AGP [b]
Elimination						
HLC $CL_{int,u}$ (µL/min/mg cytosolic protein)	10.9 [a]	1062 [a]	175 [a]	1.86 [a]	33.4 [a]	13.1 [a]
HLS9 -NADPH $CL_{int,u}$ (µL/min/mg S9 protein)	2.2 [a]	177.3 [a]	72 [a]	<1 [a]	150.6 [a]	2.8 [a]
$HLM_{,u}$ (µL/min/mg microsomal protein)	7.9 [a]	47.3 [a]	6.7 [a]	3.06 (Renwick et al., 2002)	587.8 [a]	<LOQ [a]
Renal clearance (L/h)	0.12 (Dolan et al., 1998; Tserng et al., 2003)	1.94 (Hutzler et al., 2012)	0 (Kaye et al., 1984)	-	1.65(Miceli et al., 2005)	16.4(Dalvie et al., 2013)
Biliary CL (L/h)	-	-	-	-	-	0.96 (Dalvie et al., 2013)
Predicted fm_{AO}	0.75	0.97	0.98	0.55	0.064	0.56
Observed In-vivo CL						
CL_{IV} (L/h) (plasma)	61.70 ± 22.14 (Dolan et al., 1998; Tserng	161.50 ± 42 (Hutzler	157.92 ± 34.86 (Kaye et	61.48 ± 14.53 (Rosen	22.50 ± 3.15 (Miceli et	96.39 ± 5.51 (Dalvie et

		et al., 2003)	et al., 2012)	al., 1984)	et al., 1999)	al., 2005)	al., 2013)
Population		Sim-Cancer		Sim-Healthy volunteers			
Simulation settings	Number of trials [c]	20	10	10	10	10	20
	Subject/trial	6	11	10	10	13	4
	Age range (years)	32-74	50-73	20-50	19-32	19-37	18-55
	Prop. female	0.3	0.63	0.5	0.5	0	0

When several data were available a weighted mean was calculated.

a in house data

b see text

c to ensure that the simulated population will be representative of the global population the number of trials was increased when the number of subjects per trial was low

Table 2: Comparison of intrinsic clearance data obtained for AO from literature reports, in-house measurements and retrograde scaling. Lab-specific scaling factors for 6 AO substrates.

HLC CL$_{int,u}$ (µL/min/mg cytosolic protein)	O^6-Benzylguanine	BIBX1382	Carbazeran	Zaleplon	Ziprasidone	Zoniporide
Literature	16.52 (Roy et al., 1995; Zientek et al., 2010)	860.7 (Hutzler et al., 2012)	446 (Zientek et al., 2010; Fu et al., 2013)	3.9 (Lake et al., 2002; Zientek et al., 2010)	410.3(Obach et al., 2012)	41.2 (Dalvie et al., 2010; Zientek et al., 2010; Fu et al., 2013)
Measured (this study)	10.9	1062	175	1.86	33.4	13.1
Estimated (this study [a]	109.4	3717	764	22.34	3338	33
Scaling factor (this study)	10	3.5	4.35	12	100	2.5

[a]estimated based on the PK profiles or reported CL

Table 3: Use of scaling factor from other compounds to predict the CL

REF	O^6-Benzylguanine	BIBX1382	Carbazeran	Zaleplon	Zoniporide	Average scaling factor	Observed CL	Predicted CL	**Ratio**
06-benzylguanine	x	3.5	4.35	12	2.5	**5.6**	62 ± 22	40 ± 9	**1.54**
BIBX1382	10	x	4.35	12	2.5	**7.2**	162 ± 42	154 ± 18	**1.05**
Carbazeran	10	3.5	x	12	2.5	**7.0**	158 ± 35	88 ± 11	**1.79**
Zaleplon	10	3.5	4.35	x	2.5	**5.1**	61 ± 15	32 ± 7	**1.96**
Zoniporide	10	3.5	4.35	12	x	**7.5**	96 ± 6	98 ± 13	**0.98**

The individual scaling factor are noted below the compounds, to predict the CL of a drug the average scaling factor of the other drugs was used. i.e the scalar used for 06-benzylguanine was 5.6 (average of 3.5, 4.35, 12 and 2.5).

*C_{max} = conc. at end of infusion, [&] AUC (0-4hr) to match the reported AUC; PO: Per oral; IV Intravenous; SS: Steady-state; QD: once daily, BID: Twice daily; heps, hepatocytes; SD: standard deviation; NR= not reported
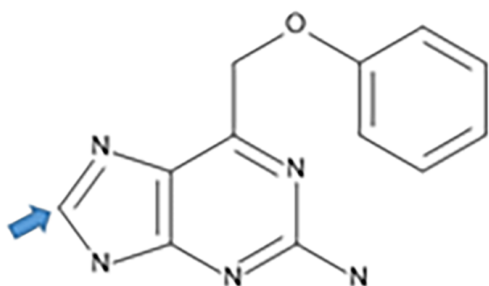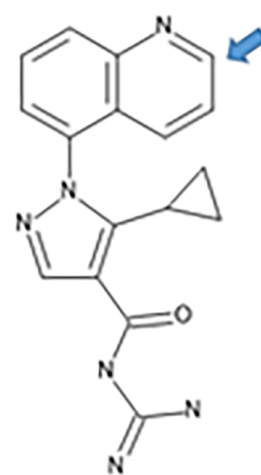
O6-benzylguanine
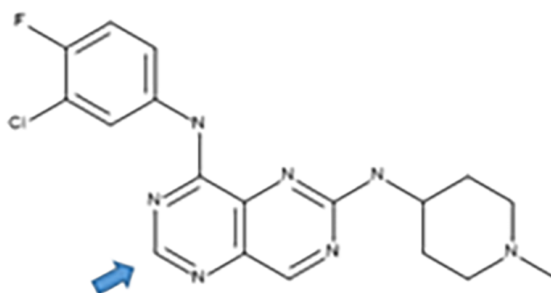
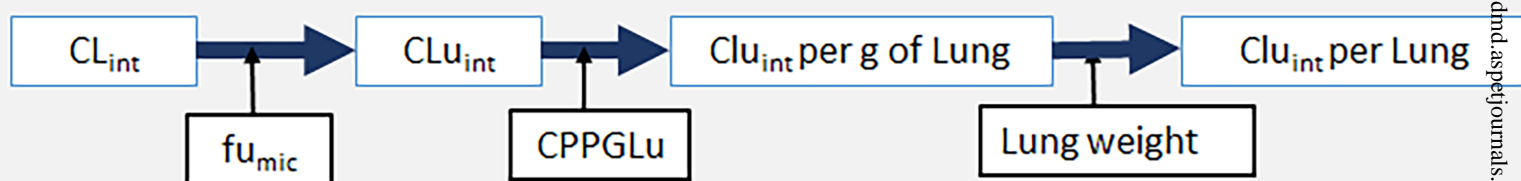**BIBX-1382**
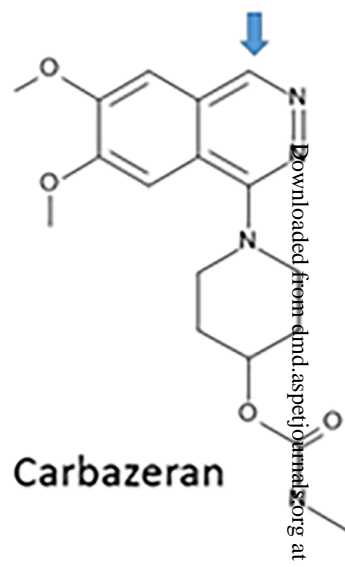
Carbazeran
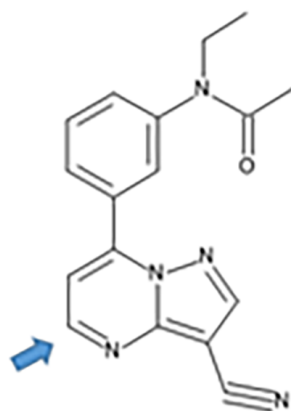
Zaleplon
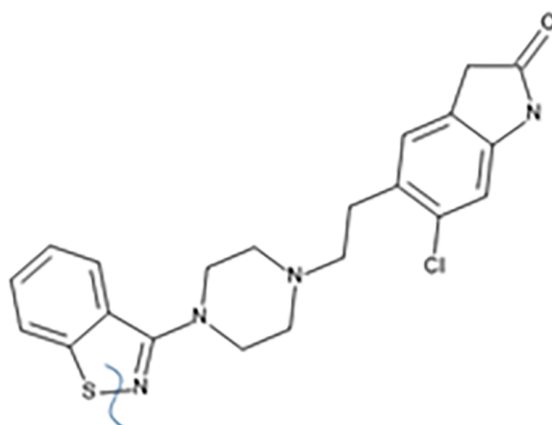
Ziprasidone
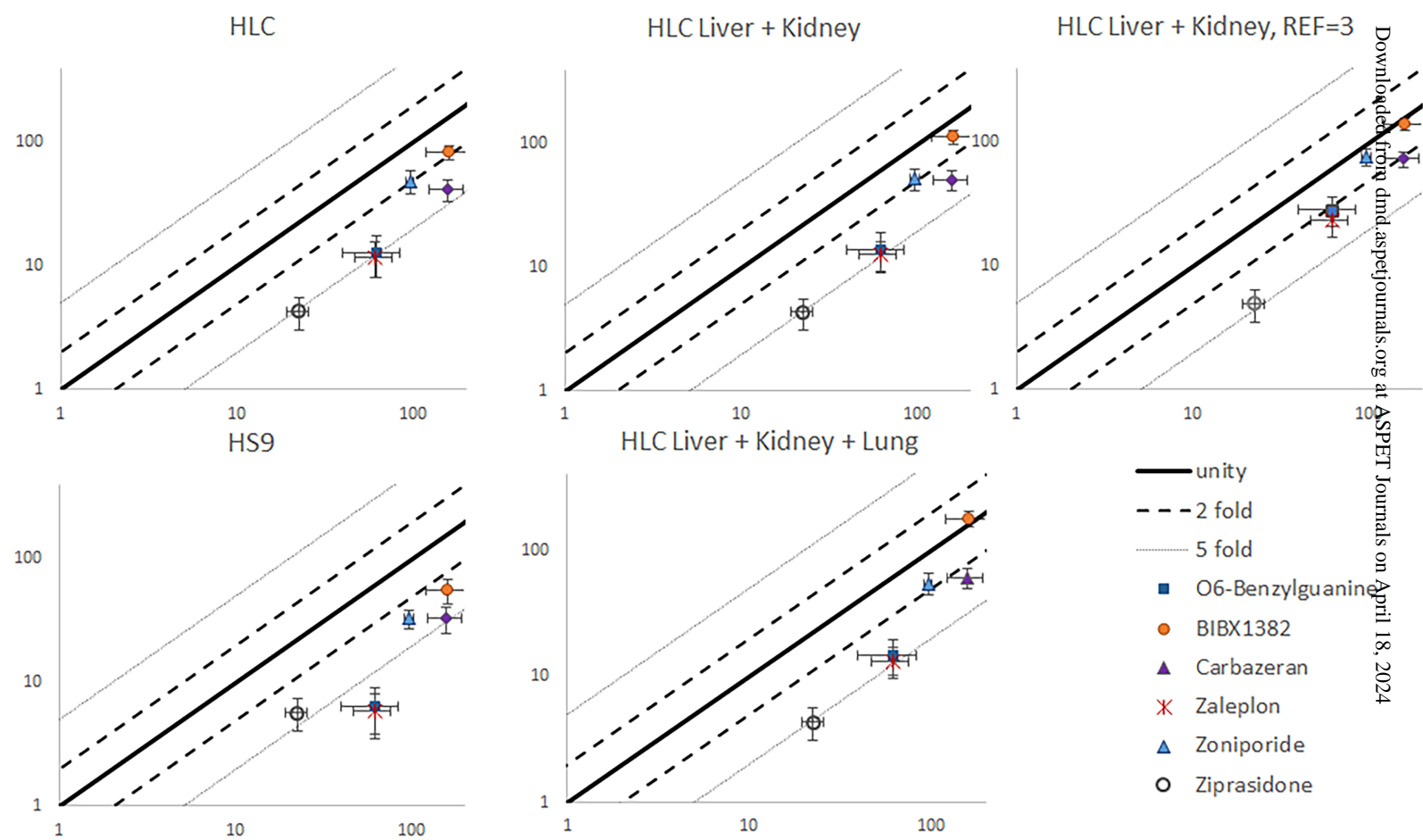*(AO cleaves bond)*

Zoniporide

$$CL_L = \frac{CLu_{int} \times fu \times CO}{CLu_{int} \times fu/B{:}P + CO}$$
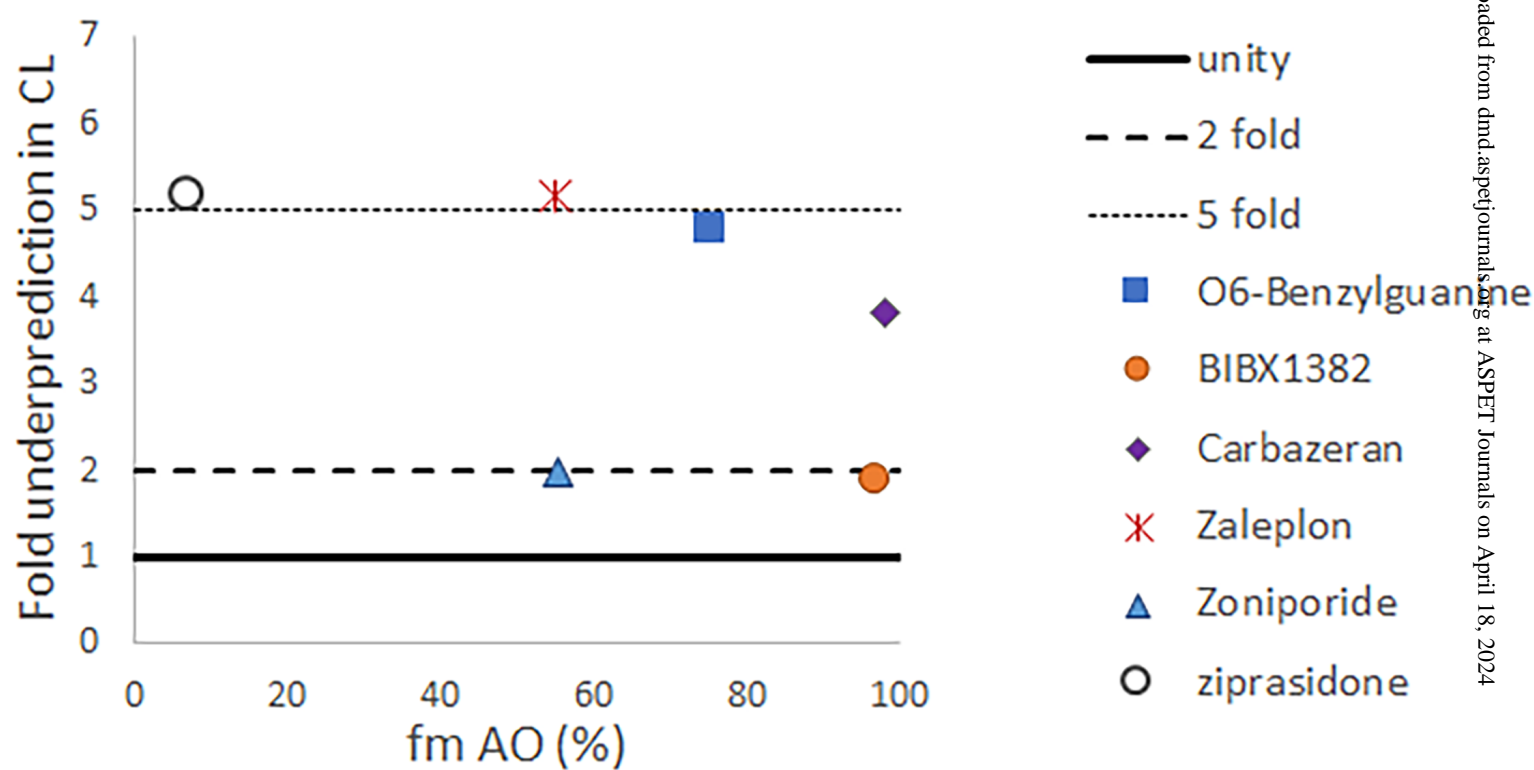
CPPGLu : cytosolic protein per gram of Lung
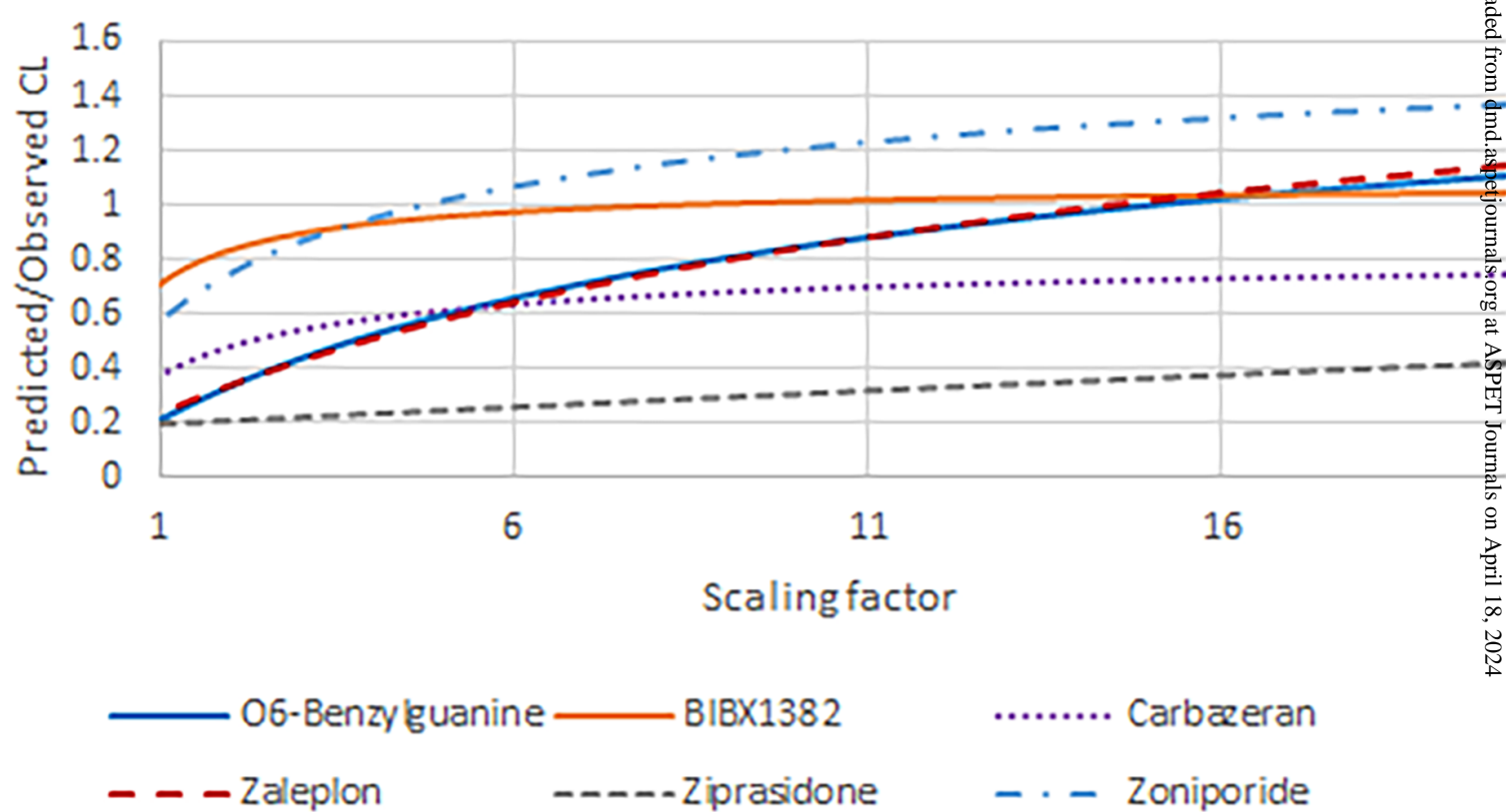
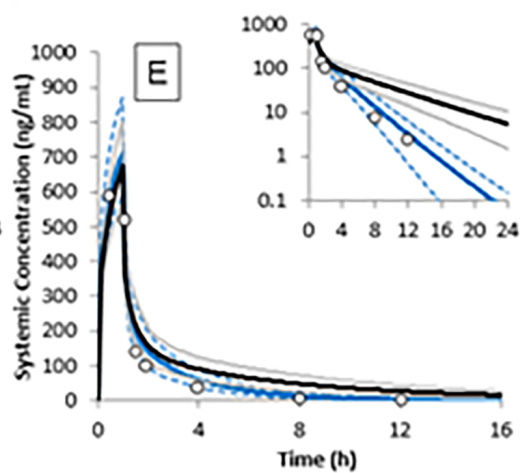CL_L : *in-vivo* hepatic AO CL

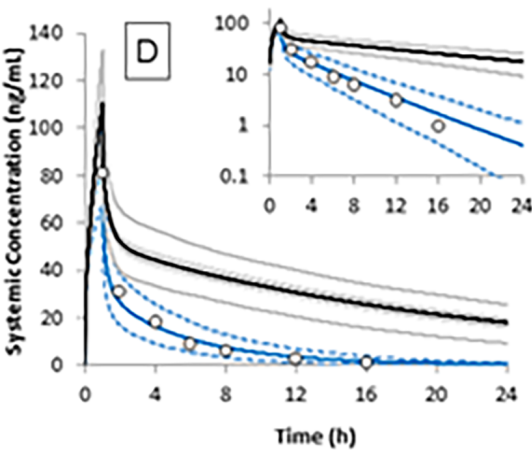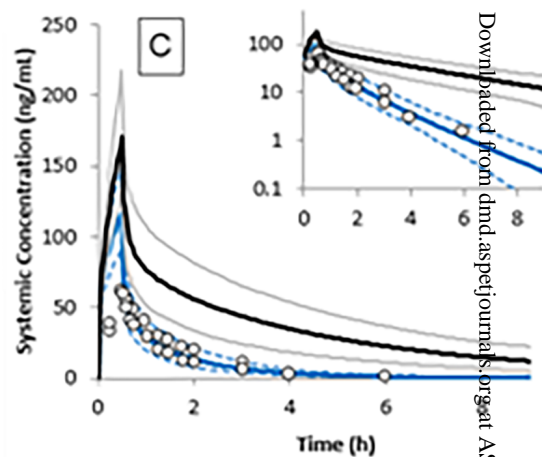CLu_{int} : free intrinsic clearance

CO: cardiac output

HLC

HLC Liver + Kidney

HLC Liver + Kidney, REF=3

HS9

HLC Liver + Kidney + Lung

— unity
-- 2 fold
····· 5 fold
■ O6-Benzylguanine
● BIBX1382
▲ Carbazeran
✳ Zaleplon
▲ Zoniporide
○ Ziprasidone

Sensitivity analyses

Predicted/Observed CL vs Scaling factor

Legend:
— O6-Benzylguanine
— BIBX1382
···· Carbazeran
- - - Zaleplon
- - - - Ziprasidone
- · - Zoniporide
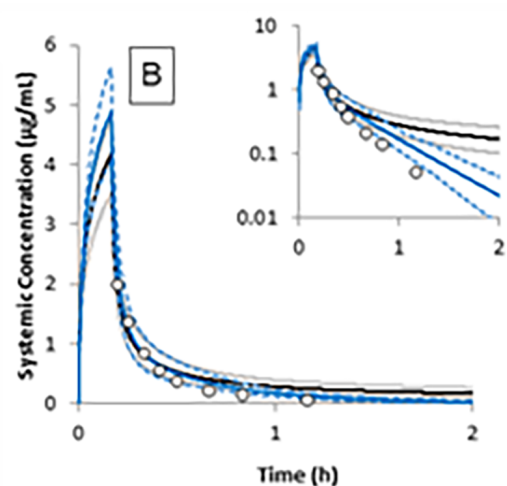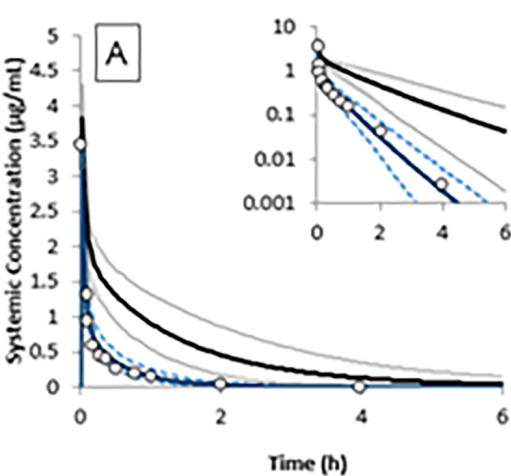
Supplemental Material

Drug Metabolism and Disposition

A laboratory specific scaling factor to predict the in vivo human clearance of aldehyde oxidase substrates

Mailys De Sousa Mendes, Alexandra Orton, Helen E. Humphries, Barry Jones, Iain Gardner, Sibylle Neuhoff, and Venkatesh Pilla Reddy

Supplementary Text

Mass Spec and HPLC system parameters:

Formic Acid System

UPLC system:	Waters Acquity BSM, SM, Column Manager and PDA
Column:	Phenomenex Kinetex C_{18} 50 x 2.1, 2.6 µm (60 °C)
Eluent:	A: Water 0.1% formic acid
	B: Methanol 0.1% formic acid
Gradient:	initial divert for 0.5 minutes
Mass spectrometer:	Waters Xevo TQ-S (serial No.- WAA673)
Ionisation mode:	electrospray ionisation (ESI) in positive-ion or negative-ion mode

Gradient	Time (min)	% A	%B
	0	95	5
	0.3	95	5
	2.2	5	95
	2.6	5	95
	2.61	95	5
	2.8	95	5
Flow	0.6 ml/min		

Supplemental Dataset 1: Simcyp workspace for 06-benzylguanine HS9.wksz

06-benzylguanine
HS9.wksz

Supplemental Dataset 2: Simcyp workspace for BIBX1382 HS9.wksz

BIBX1382 HS9.wksz

Supplemental Dataset 3: Simcyp workspace for Carbazeran HS9.wksz

carbazeran
HS9.wksz

Supplemental Dataset 4: Simcyp workspace for Zalepton hs9.wksz

zalepton hs9.wksz

Supplemental Dataset 5: Simcyp workspace for Zoniporide hs9.wksz

zoniporide
hs9.wksz

Supplemental Dataset 6: Simcyp workspace for Ziprasidone HS9.wksz

ziprasidone
HS9.wksz